

## **OPTIMIZATION OF PIN-FIN HEAT SINKS IN BYPASS FLOW USING ENTROPY GENERATION MINIMIZATION METHOD**

**Waqar A. Khan**

Associate Professor  
Department of Mathematics  
CIIT Abbottabad, NWFP, Pakistan  
Email: wkhan@ciit.net.pk

**Michael M. Yovanovich**

Distinguished Professor Emeritus  
Department of Mechanical Engineering  
University of Waterloo, Waterloo, Canada, N2L 3G1  
mmyov@uwaterloo.ca

### **ABSTRACT**

*An entropy generation minimization, EGM, method is applied to study the thermodynamic losses caused by heat transfer and pressure drop for the fluid in a cylindrical pin-fin heat sink and bypass flow regions. A general expression for the entropy generation rate is obtained by considering control volumes around heat sink and bypass regions. The conservation equations for mass and energy with the entropy balance are applied in both regions. Inside the heat sink, analytical/empirical correlations are used for heat transfer coefficients and friction factors, where the reference velocity used in Reynolds number and pressure drop is based on the minimum free area available for the fluid flow. In bypass regions theoretical models, based on laws of conservation of mass, momentum and energy, are used to predict flow velocity and pressure drop. Both in-line and staggered arrangements are studied and their relative performance is compared for the same thermal and hydraulic conditions. A parametric study is also performed to show the effects of bypass on the overall performance of heat sinks.*

### **INTRODUCTION**

Pin-fin heat sinks provide a large surface area for the dissipation of heat and effectively reduce the thermal resistance of the package at the cost of higher pumping power. They often take less space and contribute less to the weight and cost of the product. For these reasons, they are widely used in applications where heat loads are substantial and/or space is limited. They are also found to be useful in situations where the direction of

the approaching flow is unknown or may change. They are usually mounted on circuit boards where significant clearances are available on the sides and at the top. Due to higher resistance for flow through the heat sink, the approaching cooling fluid takes a detour around the heat sink, which always results in a better hydraulic performance with lesser thermal performance.

Many researchers [1-12] have conducted experiments to study the effects of side/top bypass clearance ratios on heat transfer and pressure drop in pin-fin heat sinks. Bejan [13-17] demonstrated the use of EGM for optimization in different applications. Culham and Muzychka [18], and Khan et. al [19-22] extended that use in optimizing fully shrouded heat sinks.

Following Kern and Kraus [23], Sonn and Bar-Cohen [24] and Iyengar and Bar-Cohen [25, 26] performed a least material optimization of cylindrical pin-fin, plate-fin, and triangular-fin array geometries by extending the use of least-material single fin analysis to multiple fin arrays. Bar-Cohen and Jelinek [27] developed guidelines and design equations for optimum plate-fin arrays.

It is obvious from the literature survey that all optimization studies, related to cylindrical pin-fin heat sinks, are limited to the optimization of fully shrouded heat sinks. The authors could not find any study related to optimization of pin-fin heat sinks in bypass flow. In this study, all relevant design parameters for pin-fin heat sinks, including clearance ratios, geometric parameters, and flow conditions are optimized simultaneously by minimizing dimensionless entropy generation rate  $Ns$  subject to manufacturing and design constraints.

## NOMENCLATURE

$A_b$	Area of the base plate $\equiv L \times W_2$ , $m^2$
$A_f$	Frontal face area of heat sink, $m^2$
$a$	Dimensionless longitudinal pitch $\equiv S_L/D$
$b$	Dimensionless transverse pitch $\equiv S_T/D$
$c$	Dimensionless diagonal pitch $\equiv S_D/D$
$C_1, C_2$	Constants defined in Eq. (3)
$CL_s$	Side clearance ratio $\equiv 2W_1/W_2$
$CL_t$	Top clearance ratio $\equiv H_2/H_1$
$c$	Dimensionless diagonal pitch $\equiv S_D/D$
$D$	Pin diameter, $m$
$D_h$	Hydraulic diameter, $m$
$f$	Friction factor
$g, l$	equality and inequality constraints
$G$	Volume flow rate, $m^3/s$
$H$	Height of duct, $m$
$h$	Average heat transfer coefficient, $W/m^2 \cdot K$
$j$	number of imposed constraints
$K_c$	Correction factor defined in Eq. (23)
$K_1, K_2, K_3$	Constants defined in Eq. (5)
$k$	Thermal conductivity, $W/m \cdot K$
$k_c, k_e$	Contraction and expansion coefficients
$\mathcal{L}$	Lagrangian function
$L$	Length of heat sink in flow direction, $m$
$\dot{m}$	mass flow rate, $kg/s$
$m$	Fin performance parameter defined in Eq. (16), $m^{-1}$
$N$	Total number of pins in heat sink $\equiv N_T N_L$
$N_L$	Number of pins in longitudinal direction
$N_T$	Number of pins in transverse direction
$Nu_D$	Nusselt number based on pin diameter $\equiv Dh/k_f$
$N_s$	dimensionless entropy generation rate
$P$	Pressure, $Pa$
$Pr$	Prandtl number $\equiv \nu/\alpha$
$Q$	Total heat transfer rate, $W$
$R_c$	Contact resistance between fins and the baseplate, $K/W$
$R_{film}$	Thermal resistance of exposed (unfinned) surface of the baseplate, $K/W$
$R_{fin}$	Resistance of a fin, $K/W$
$R_m$	Material resistance of the baseplate, $K/W$
$Re_D$	Reynolds number based on pin diameter $\equiv DU_{max}/\nu$
$Re_{D_h}$	Reynolds number based on hydraulic diameter $\equiv D_h U/\nu$
$S_D$	Diagonal pitch, $m$
$S_L$	Longitudinal distance between two consecutive pins, $m$
$S_T$	Transverse distance between two consecutive pins, $m$
$T$	Temperature, $K$
$t_b$	Thickness of baseplate, $m$

$U$	Velocity, $m/s$
$U_{app}$	Approach velocity, $m/s$
$U_{max}$	Maximum velocity in minimum flow area, $m/s$
$W$	Width of duct, $m$
$W_2$	Width of heat sink, $m$

### Greek Symbols

$\Delta P$	Pressure drop, $Pa$
$\eta_{fin}$	Fin efficiency $\equiv \tanh(mH_{fin})/(mH_{fin})$
$\gamma$	aspect ratio $\equiv H_{fin}/D$
$\mu$	Absolute viscosity of fluid, $kg/m \cdot s$
$\nu$	Kinematic viscosity of fluid, $m^2/s$
$\rho$	Fluid density, $kg/m^3$

### Subscripts

1	Side bypass
2	Top bypass
$a$	Ambient
$b$	Base plate or unfinned surface of baseplate
$d$	Duct
$f$	Fluid
$fin$	Single fin
$fins$	All fins with exposed base plate area
$hs$	Heat sink
$m$	Bulk material
$T$	Thermal
$w$	Wall

## ANALYSIS

The front, side and top views of an in-line pin-fin heat sink are shown in Fig. 1. The dimensions of the baseplate are  $W_2 \times L \times t_b$ , where  $W_2$  is the width of the heat sink,  $L$  is the length measured in the downstream direction and  $t_b$  is the thickness of the base plate. The dimensions of the duct are  $W \times H$ , where  $W$  is the width and  $H$  is the height of the duct. The dimensions of the side bypass are  $W_1 \times H_1$ , where as the dimensions of the top bypass are  $W \times H_2$ . Flow in side and top bypass regions is assumed as inviscid flow. The pin-fins can be arranged in in-line or staggered manner.

Each pin fin has diameter  $D$  and height  $H_{fin}$ . The dimensionless longitudinal and transverse pitches are  $a = S_L/D$  and  $b = S_T/D$ . The source of heat is applied to the bottom of the heat sink. The flow is assumed to be laminar, steady, and two dimensional. The duct velocity of the fluid is  $U_d$  and the ambient temperature is  $T_a$ . There is no leakage of fluid from the top or sides. The wall temperature of the pin is  $T_w (> T_a)$  and the baseplate temperature is  $T_b$ . The side and top clearance ratios are defined as

$$\left. \begin{aligned} CL_s &= \frac{2W_1}{W_2} \\ CL_t &= \frac{H_2}{H_1} \end{aligned} \right\} \quad (1)$$

Khan et al. ([19] used law of conservation of mass and energy and obtained the expressions for the average velocities in side bypass, top bypass and just in front of heat sink regions.

$$\left. \begin{aligned} U_1 &= \frac{C_2 U_d}{a_1 C_2 + a_2 C_1 + a_f C_1 C_2} \\ U_2 &= \frac{C_1 U_d}{a_1 C_2 + a_2 C_1 + a_f C_1 C_2} \\ U_{app} &= \frac{C_1 C_2 U_d}{a_1 C_2 + a_2 C_1 + a_f C_1 C_2} \end{aligned} \right\} \quad (2)$$

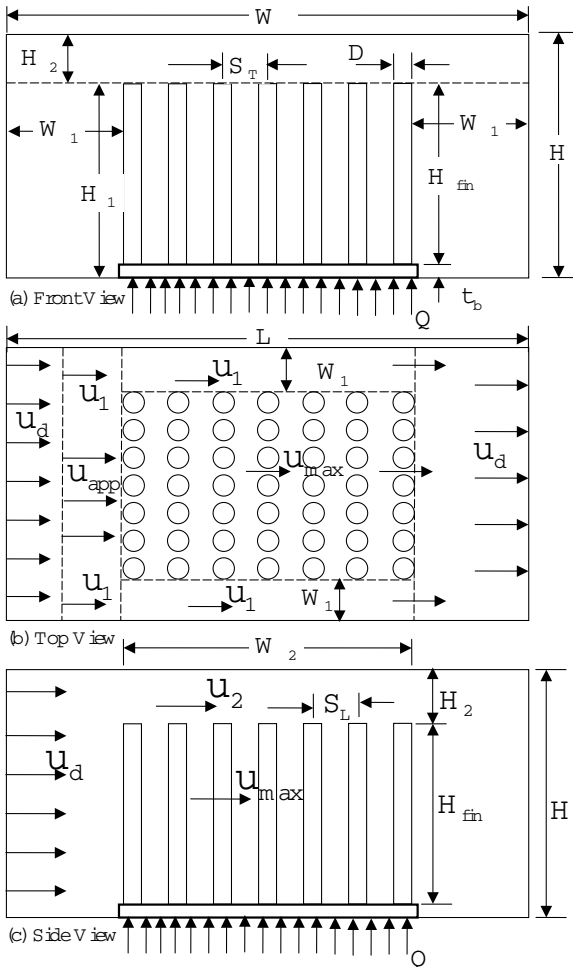


Fig. 1 Front, Top and Side Views of an In-Line Pin-Fin Heat Sink in Bypass Flow.

where

$$\left. \begin{aligned} C_1 &= \sqrt{\frac{1+K_1}{1+\sigma_3^2 K_3}} \\ C_2 &= \sqrt{\frac{1+K_2}{1+\sigma_3^2 K_3}} \end{aligned} \right\} \quad (3)$$

and

$$\left. \begin{aligned} a_1 &= \frac{A_1}{A_d} \\ a_2 &= \frac{A_2}{A_d} \\ a_f &= \frac{A_f}{A_d} \end{aligned} \right\} \quad (4)$$

with

$$\left. \begin{aligned} K_1 &= f_1 \frac{L}{Dh_1} \\ K_2 &= f_2 \frac{L}{Dh_2} \\ K_3 &= f_3 (k_c + k_e + f_3 N_L) \end{aligned} \right\} \quad (5)$$

## MODEL DEVELOPMENT

In the heat sink region, the entropy generation associated with heat transfer and frictional effects serve as a direct measure of the ability to transfer heat to the surrounding cooling medium. In the bypass regions, entropy generation is associated with the fluid flow only. A model that establishes a relationship between the total entropy generation rate and heat sink design parameters can be optimized in such a manner that all relevant design conditions combine to produce the best possible heat sink for the given constraints. The total entropy generation rate can be written as

$$\dot{S}_{gen} = \dot{S}_{gen,hs} + \dot{S}_{gen,bp} \quad (6)$$

where the entropy generation rate in the heat sink can be obtained by following Bejan [28] and Khan et. al [20-22] and applying the laws of conservation of mass and energy with the entropy balance and can be written as

$$\dot{S}_{gen,hs} = \left( \frac{Q^2}{T_a T_{bp}} \right) R_{hs} + \frac{\dot{m} \Delta P_{hs}}{\rho T_a} \quad (7)$$

Similarly, the entropy generation rate in the bypass region due to fluid flow can be written as

$$\dot{S}_{gen,bp} = \frac{\dot{m}\Delta P_{bp}}{\rho T_a} \quad (8)$$

where  $\Delta P_{bp}$  is the total pressure drop in the bypass regions and can be written as

$$\Delta P_{bp} = 2\Delta P_1 + \Delta P_2 \quad (9)$$

with

$$\left. \begin{aligned} \Delta P_1 &= \left( \frac{1}{2} \rho U_1^2 \right) f_1 (L/D_{h1}) \\ \Delta P_2 &= \left( \frac{1}{2} \rho U_2^2 \right) f_2 (L/D_{h2}) \end{aligned} \right\} \quad (10)$$

where  $f_1$  and  $f_2$  are the friction factors in the side and top bypass regions and are given by

$$f_1 = \frac{24}{Re_{D_{h1}}} \quad \text{and} \quad f_2 = \frac{24}{Re_{D_{h2}}} \quad (11)$$

This assumes fully-developed flow between parallel plates. Equation (11) shows that the entropy generation rate in the heat sink depends on the heat sink resistance and the pressure drop across the heat sink, provided that the heat load, mass flow rate and ambient conditions are specified. The lumped heat sink resistance is given by:

$$R_{hs} = R_m + R_{fins} \quad (12)$$

where  $R_m$  is the bulk material resistance, given by:

$$R_m = \frac{t_{bp}}{kA} \quad (13)$$

and  $R_{fins}$  is the overall resistance of the fins and the exposed base plate, which can be written as:

$$R_{fins} = \frac{1}{\frac{N}{R_c + R_{fin}} + \frac{1}{R_{bp}}} \quad (14)$$

where

$$\left. \begin{aligned} R_c &= \frac{1}{h_c A_c} \\ R_{fin} &= \frac{1}{h_{fin} A_{fin} \eta_{fin}} \\ R_{bp} &= \frac{1}{h_{bp} A_{bp}} \end{aligned} \right\} \quad (15)$$

with

$$\left. \begin{aligned} \eta_{fin} &= \frac{\tanh(mH)}{mH} \\ m &= \sqrt{\frac{4h_{fin}}{kD}} \end{aligned} \right\} \quad (16)$$

Khan [28] developed the following analytical correlation for the dimensionless heat transfer coefficient for the cylindrical fin array:

$$Nu_{D_{fin}} = \frac{h_{fin} D}{k_f} = C_3 Re_D^{1/2} Pr^{1/3} \quad (17)$$

where  $C_3$  is a constant which depends on the longitudinal and transverse pitches, arrangement of the pins, and thermal boundary conditions. For isothermal boundary condition, it is given by:

$$C_3 = \begin{cases} [0.2 + \exp(-0.55a)] b^{0.285} a^{0.212} & \text{In-Line arrangement} \\ \frac{0.61 b^{0.091} a^{0.053}}{[1 - 2\exp(-1.09a)]} & \text{Staggered arrangement} \end{cases} \quad (18)$$

The heat transfer coefficient for the base plate,  $h_{bp}$ , can be determined by considering it a finite plate. Khan [28] developed the following analytical correlation for dimensionless heat transfer coefficient for a finite plate:

$$Nu_L = \frac{h_{bp} L}{k_f} = 0.75 Re_L^{1/2} Pr^{1/3} \quad (19)$$

where  $L$  is the length of the base plate in the streamwise direction. The mass flow rate through the pins is given by:

$$\dot{m} = \rho U_{app} N_T b H_{fin} D \quad (20)$$

The pressure drop associated with flow across the pin fins is given by:

$$\Delta P_{hs} = f_3 \frac{\rho U_{max}^2}{2} N_L \quad (21)$$

where the friction factor  $f$  depends on the Reynolds number and the array geometry, and it can be written as:

$$f_3 = \begin{cases} K_c [0.233 + 45.78/(b-1)^{1.1} Re_D] & \text{In-Line arrangement} \\ K_c [378.6/b^{13.1/b}] / Re_D^{0.68/b^{1.29}} & \text{Staggered arrangement} \end{cases} \quad (22)$$

where  $K_c$  is a correction factor depending upon the flow geometry and arrangement of the pins. It is given by:

$$K_c = \begin{cases} 1.009 \left( \frac{b-1}{a-1} \right)^{1.09/Re_D^{0.553}} & \text{In-Line arrangement} \\ 1.175(a/b Re_D^{0.3124}) + 0.5 Re_D^{0.0807} & \text{Staggered arrangement} \end{cases} \quad (23)$$

All the correlations for friction and correction factors are derived from graphs given in Žukauskas [29]. The velocity  $U_{max}$ , in Eq. (21), represents the maximum average velocity seen by the array as flow accelerates between pins, and is given by:

$$U_{max} = \max \left\{ \frac{b}{b-1} U_{app}, \frac{b}{c-1} U_{app} \right\} \quad (24)$$

where  $c = \sqrt{a^2 + (b/2)^2}$  is the dimensionless diagonal pitch.

The dimensionless entropy generation rate can be written as

$$Ns = \dot{S}_{gen} / (Q^2 U_{max} / k_f \nu T_a^2) \quad (25)$$

## OPTIMIZATION PROCEDURE

The problem considered in this study is to minimize the dimensionless entropy generation rate, given by Eq. (7), for the optimal overall performance of the tube bank. If  $f(\mathbf{x})$  represents the dimensionless entropy generation rate that is to be minimized subject to equality constraints  $g_j(x_1, x_2, \dots, x_n) = 0$  and inequality constraints  $l_k(x_1, x_2, \dots, x_n) \geq 0$ , then the complete mathematical formulation of the optimization problem may be written in the following form:

$$\text{minimize } f(\mathbf{x}) = N_s(\mathbf{x}) \quad (26)$$

subject to the equality constraints

$$g_j(\mathbf{x}) = 0, \quad j = 1, 2, \dots, m \quad (27)$$

and inequality constraints

$$l_j(\mathbf{x}) \geq 0, \quad j = m+1, \dots, n \quad (28)$$

The objective function can be redefined by using Lagrangian function as follows:

$$\mathcal{L}(\mathbf{x}, \lambda, \chi) = f(\mathbf{x}) + \sum_{j=1}^m \lambda_j g_j(\mathbf{x}) - \sum_{j=m+1}^n \chi_j l_j(\mathbf{x}) \quad (29)$$

where  $\lambda_j$  and  $\chi_j$  are the Lagrange multipliers. The  $\lambda_j$  can be positive or negative but the  $\chi_j$  must be  $\geq 0$ . The necessary condition for  $\mathbf{x}^*$  to be a local minimum of the problem, under consideration, is that the Hessian matrix of  $\mathcal{L}$  should be positive semidefinite, i.e.,

$$\mathbf{v}^T \nabla^2 [\mathcal{L}(\mathbf{x}^*, \lambda^*, \chi^*)] \mathbf{v} \geq 0 \quad (30)$$

For a local minimum to be a global minimum, all the eigenvalues of the Hessian matrix should be  $\geq 0$ .

A system of non-linear equations is obtained, which can be solved using numerical methods such as a multivariable Newton-Raphson method. This method has been described in Stoecker [30] and applied by Culham and Muzychka [31], and Khan et al. [22] to study the optimization of plate or pin fin heat sinks. In this study, the same approach is used to optimize the overall performance of a tube bank in such a manner that all relevant design conditions combine to produce the best possible tube bank for the given constraints. The optimized results are then compared for in-line and staggered arrangements.

A simple procedure was coded in MAPLE 10, a symbolic mathematics software, which solves the system of  $N$  non-linear equations using the multivariable Newton-Raphson method. Given, the Lagrangian  $L$ , the solution vector  $[\mathbf{x}]$ , initial guess  $[\mathbf{x}_0]$ , and maximum number of iterations  $N_{max}$ , the procedure systematically applies the Newton-Raphson method until the desired convergence criteria and/or maximum number of iterations is achieved. The method is quite robust provided an adequate initial guess is made.

## RESULTS AND DISCUSSION

The parameters given in Table 1 are used as the default case to determine the thermal and hydraulic resistances and entropy generation rate for both in-line and staggered pin-fin heat sinks in bypass flow. The air properties are evaluated at the ambient temperature.

The effect of side and top clearance ratio on thermal resistance and total pressure drop is shown in Fig. 2. In each case, the

Table 1. ASSUMED PARAMETRIC VALUES IN BYPASS FLOW

Quantity	Parameter Values
Footprint ( $mm^2$ )	$50 \times 50$
Source Dimensions ( $mm^2$ )	$50 \times 50$
Baseplate Thickness ( $mm$ )	2
Pin Diameter ( $mm$ )	4
Overall Height of Heat Sink ( $mm$ )	50
Duct Flow Rate ( $m^3/s$ )	0.01
Thermal Conductivity of Solid ( $W/m \cdot K$ )	210
Thermal Conductivity of Fluid ( $W/m \cdot K$ )	0.026
Thermal Contact Conductance ( $W/m^2 \cdot K$ )	$10^4$
Density of Fluid ( $kg/m^3$ )	1.1614
Specific Heat of Fluid ( $J/kg \cdot K$ )	1007
Kinematic Viscosity ( $m^2/s$ )	$1.58 \times 10^{-5}$
Prandtl Number	0.71
Heat Load ( $W$ )	10
Ambient Temperature ( $^{\circ}C$ )	27

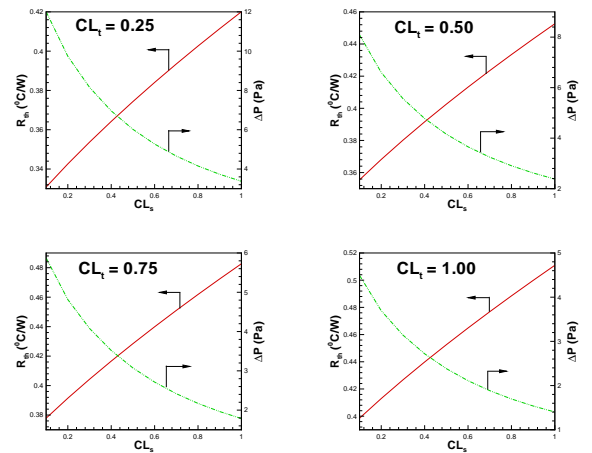


Fig. 2 THERMAL RESISTANCE AND PRESSURE DROP IN SIDE AND TOP BYPASS FLOWS.

Figure 4 shows the effects of pin diameter and side clearance ratios on the dimensionless entropy generation rate for an in-line arrangement. It is obvious from the figure that for a fixed top clearance ratio, the dimensionless entropy generation rate decreases with increase in side clearance ratio and decrease in pin diameter. In the in-line arrangement, with the decrease in pin diameter, the heat transfer surface area decreases that allows the increase in pressure drop keeping the longitudinal or transverse pitch ratios fixed.

The effect of pin height on the dimensionless entropy generation rate is shown in Fig. 5 for an in-line arrangement. For each pin height, optimum entropy generation rate and optimum Reynolds number exist which decrease with decrease in pin height and increase in Reynolds number based on pin diameter and the maximum velocity  $U_{max}$  within the pin-fins.

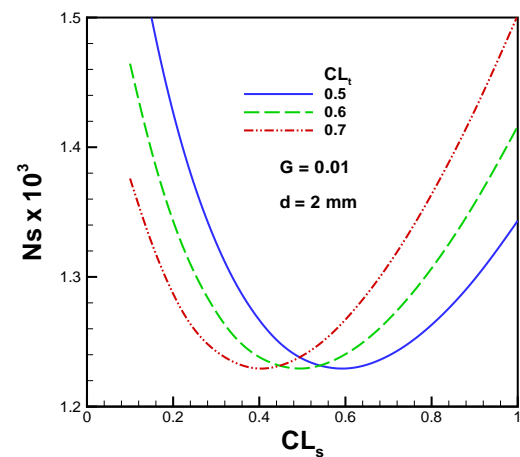
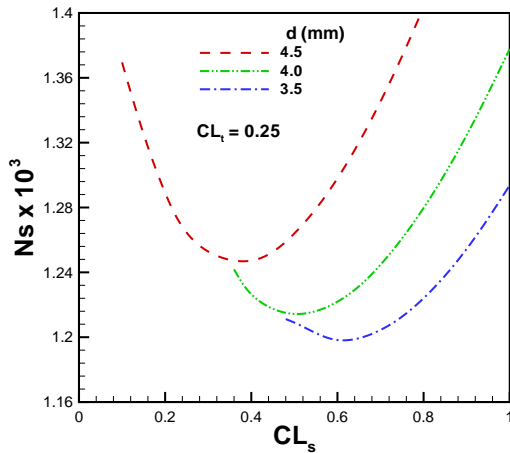


Fig. 3 DIMENSIONLESS ENTROPY GENERATION RATE VS SIDE AND TOP CLEARANCE.

thermal resistance is increasing while pressure drop is decreasing with the increase in side and/or top clearance ratios respectively. It is due to the fact that with the increase in side or top clearance ratio, pressure drop in the heat sink decreases whereas thermal resistance increases since the effective resistance for the flow decreases. Note that for  $CL_s = 0$  and  $CL_t = 0$ , the entire flow goes through the heat sink and the total thermal resistance of the heat sink is minimum. Thus, the thermal resistance is a direct measure of the deterioration of the thermal performance due to the presence of side and top bypass regions around the heat sink. However, with both side and top clearance ratios, the thermal performance increases further. In each case, the optimum point (where  $R_{th}$  and  $\Delta P$  intersect) increases with the increase in  $CL_t$  but remain fixed for  $CL_s$ . The effect of side and top clearance on the dimensionless entropy generation rate is shown in Fig. 3 for fixed pin diameter and volume flow rate. The optimum entropy generation rate remains constant with the increase in side clearance and decrease in top clearance. It is due to the complex behavior of the entropy generation rate due to increase/decrease in side/top clearance ratios.



**Fig. 4 DIMENSIONLESS ENTROPY GENERATION RATE Vs SIDE CLEARANCE FOR DIFFERENT PIN DIAMETERS.**

It was observed that  $U_{max}$  is maximum, when the top clearance ratio is zero and decreases with increase in  $CL_t$ . The effect of side clearance ratio on thermal resistance and total pressure drop in both in-line and staggered arrangements is shown in Fig. 6 for a fixed top clearance ratio. As expected, in both arrangements, the thermal resistance increases and pressure drop decreases with increase in side clearance ratio. For a fully shrouded heat sink (i.e.,  $CL_s = 0$  and  $CL_t = 0$ ), the pressure drop is maximum whereas thermal resistance is minimum. Pressure drop in the heat sink decreases with an increase in the side clearance ratio since the effective resistance for the flow decreases. The staggered arrangement shows higher pressure drop in the heat sink and lower thermal resistance for any  $CL_s$ .

The effects of pin height on the performance of cylindrical pin-fin heat sinks in side bypass flow are shown in Fig. 7 for both arrangements. The optimum dimensionless entropy generation rate decreases with the decrease in pin heights for both arrangements. The in-line arrangement performs much better for all three cases. The optimum Reynolds number increases with a decrease in pin height for both arrangements. Figure 7 also shows the effects of Reynolds number on the performance of heat sinks in side bypass flow for both arrangements. For different pin heights, in-line arrangements give better performance for higher Reynolds numbers and smaller pin heights.

## Conclusions

An optimal design of cylindrical pin-fin heat sinks in side and top bypass flows is obtained for both the in-line and staggered arrangements. The effects of side and top clearance ratios, pin diameter, pin height, and Reynolds numbers are examined with respect to their roles in influencing optimum design condi-

tions and the overall performance of the pin-fin heat sink. It is demonstrated that

1. Thermal resistance increases whereas pressure drop decreases with increase in side and/or top clearance ratios.
2. The dimensionless entropy generation rate decreases with increase in side/top clearance ratio and decrease in pin diameter.
3. The optimum dimensionless entropy generation rate and Reynolds numbers decrease with decrease in pin height.
4. The staggered arrangement shows higher pressure drop and lower thermal resistance for any clearance ratio.
5. The in-line arrangement shows better performance for any pin height and side/top clearance ratio.

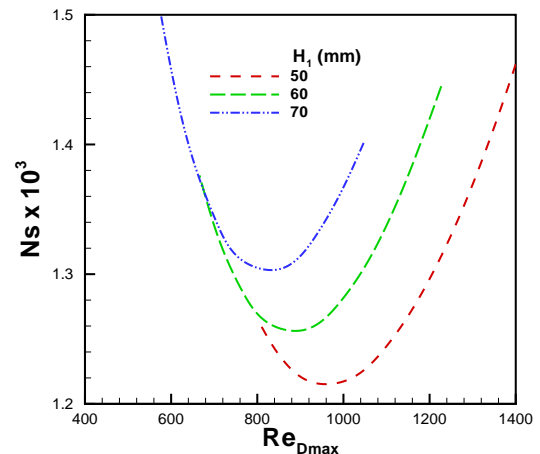


**Fig. 5 DIMENSIONLESS ENTROPY GENERATION RATE Vs SIDE CLEARANCE FOR DIFFERENT PIN HEIGHTS.**

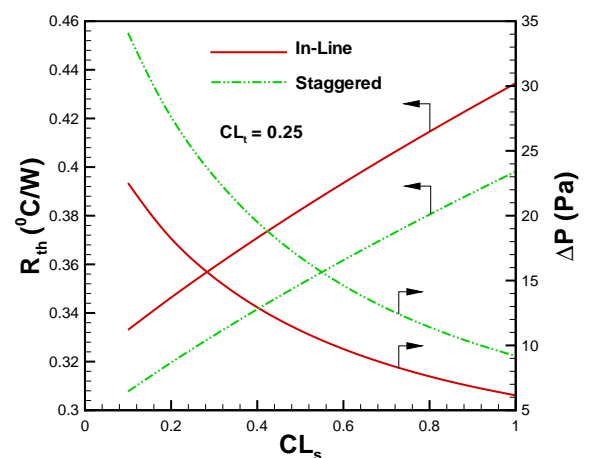


**Fig. 6 COMPARISON OF THERMAL RESISTANCE AND PRESSURE DROP FOR IN-LINE AND STAGGERED**

## ARRANGEMENTS.

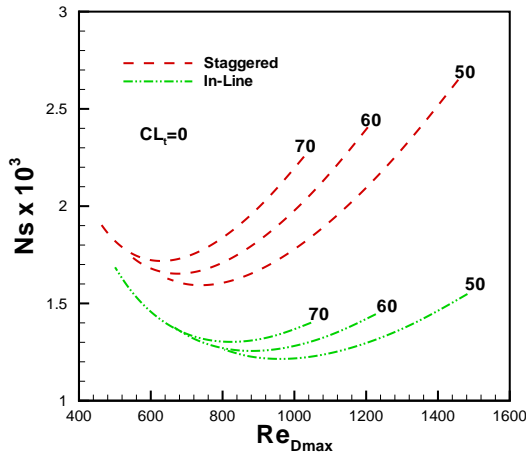


**Fig. 7 COMPARISON OF DIMENSIONLESS ENTROPY GENERATION RATE IN-LINE AND STAGGERED ARRANGEMENTS.**

## ACKNOWLEDGMENTS

The authors gratefully acknowledge the financial support of Natural Sciences and Engineering Research Council of Canada and the Center for Microelectronics Assembly and Packaging.

## REFERENCES

1. Lei, N. and Ortega, A., Experimental hydraulic characterization of pin fin heat sinks with top and side bypass, Ninth Intersociety Conference on Thermal and Thermomechanical Phenomena in Electronic Systems, Jun 1-4 2004, Las Vegas, NV, United States, Vol. 1, pp. 418-428, 2004.
2. Urdaneta, M., Ortega, A., Westphal, R. V., Experiments and Modeling of the Hydraulic Resistance of In-Line Square Pin Fin Heat Sinks with Top Bypass Flow, Advances in Electronic Packaging, International Electronic Packaging Technical Conference and Exhibition, Jul 6-11 2003, Maui, HI, United States, Vol. 2, pp. 587-596, 2003.
3. Urdaneta, M. and Ortega, A., Experiments and Modeling of the Thermal Resistance of In-Line Square Pin-Fin Heat Sinks with Top Bypass flow, Advances in Electronic Packaging, International Electronic Packaging Technical Conference and Exhibition, Jul 6-11 2003, Maui, HI, United States, Vol. 2, 2003, pp. 597-604.
4. Dogruoz, M. B., Urdaneta, M., Ortega, A., Experiments and Modeling of the Heat Transfer of In-Line Square Pin-Fin heat Sinks with Top Bypass Flow, American Society of Mechanical Engineers, Heat Transfer Division, ASME International Mechanical Engineering Congress and Exposition,

Nov 17-22 2002, New Orleans, LA, United States, Vol. 372, No. 7, 2002, pp. 195-206.

5. Shaukatullah, H., Storr, W. R., Hansen, B. J., and Gaynes, M. A., Design and Optimization of Pin Fin Heat Sinks for Low Velocity Applications, IEEE Transactions on Components, Packaging, and Manufacturing Technology, Part A, Vol. 19, No. 4, pp. 486-494, 1996.
6. Rizzi, M., Catton, I., An Experimental Study of Pin Fin Heat Sinks and Determination of End Wall Heat Transfer, Proceedings of the ASME Summer Heat Transfer Conference, Jul 21-23 2003, Las Vegas, NV, United States, Vol. 2003, pp. 445-452
7. Rizzi, M., Canino, M., Hu, K., Jones, S., Travkin, V., and Catton, I., Experimental Investigation of Pin Fin Heat Sink Effectiveness, Proceedings of the National Heat Transfer Conference, Anaheim, CA, United States, Jun 10-12, Vol. 2, pp. 1235-1243, 2001.
8. Jonsson, H., Moshfegh, B., Modeling of the Thermal and Hydraulic Performance of Plate Fin, Strip Fin, and Pin Fin Heat Sinks - Influence of Flow Bypass, IEEE Transactions on Components and Packaging Technologies, Vol. 24, No. 2, pp. 142-149, , 2001.
9. Jonsson, H. and Moshfegh, B., Modeling of the Thermal and Hydraulic Performance of Plate Fin, Strip Fin, and Pin Fin Heat Sinks - Influence of Flow Bypass, 7th Intersociety Conference on Thermal and Thermomechanical Phenomena in Electronic Systems-ITherm 2000, May 23-May 26 2000, Las Vegas, NV, USA, Vol. 1, pp. 185-192, , 2000.
10. Jonsson, H. and Moshfegh, B., Enhancement of the Cooling Performance of Circular Pin Fin Heat Sinks Under Flow Bypass Conditions, Thermomechanical Phenomena in Electronic Systems, 8th Intersociety Conference on Thermal and Thermomechanical phenomena in Electronic Systems, May 30-Jun 1 2002, San Diego, CA, United States, 2002, pp. 425-432.
11. Jonsson, H. and Moshfegh, B., CFD Modeling of the Cooling Performance of Pin Fin Heat Sinks Under Bypass Flow Conditions, Advances in Electronic Packaging, Pacific Rim/International, Intersociety Electronic Packaging Technical/Business Conference and Exhibition, Jul 8-13 2001, Kauai, HI, United States, Vol. 1, 2001, pp. 393-403.
12. Chapman, C. L., Lee, S., and Schmidt, B. L., Thermal performance of an Elliptical Pin Fin Heat Sink, Proceedings of the 10th IEEE Semiconductor Thermal Measurement and Management Symposium, Feb 1-3, 1994, San Jose, CA, USA, pp. 24-31, 1994.
13. Bejan, A., Entropy Generation Minimization, CRC Press, New York, 1996.
14. A. Bejan, 2001, "Thermodynamic Optimization of Geometry in Engineering Flow Systems," Exergy Int. J. 1(4), pp. 269-277.
15. A. Bejan, 1978, "General Criterion for Rating Heat-



- Exchanger Performance," *Int J. Heat and Mass Transfer*, Vol. 21, pp. 655-658.
16. A. Bejan, ,1996, "Entropy Generation Minimization: The New Thermodynamics of Finite-Size Devices and Finite-Time Processes," *Journal of Applied Physics*, Vol. 79, No.3, pp.1191-1218.
  17. A. Bejan, 2002, "Fundamentals of Exergy Analysis, Entropy generation Minimization, and the Generation of flow Architecture," *International Journal of Energy Research*, Vol. 26, pp.545-565.
  18. Culham, R. J. and Muzychka, Y. S., Optimization of Plate Fin Heat Sinks Using Entropy Generation Minimization, *IEEE Transactions on Components and Packaging Technologies*, Vol. 24, No. 2, pp. 159-165, 2001.
  19. Khan, W. A., Yovanovich, M. M., and Culham, J. R., "Effect of Bypass on Overall Performance of Pin Fin Heat Sinks," presented at 9th AIAA/ASME Joint Thermophysics and Heat Transfer Conference, Hyatt Regency, San Francisco, California, USA, 5-8 June, 2006. Also accepted for publication in *AIAA Journal of Thermophysics and Heat Transfer* (in press)
  20. Khan, W. A., Yovanovich, M. M., and Culham, J. R., "Optimization of Microchannel Heat Sinks Using Entropy Generation Minimization Method," presented at Semiconductor Thermal Measurement and Management Symposium, Intercontinental Hotel, Dallas TX USA March 14-16, 2006. Also accepted for publication in *IEEE Transactions on Components and Packaging Technologies* (in press).
  21. Khan, W. A., Culham, J. R., and Yovanovich, M. M., "Optimal Design of Tube Banks in Crossflow Using Entropy Generation Minimization Method," presented at 44th AIAA Aerospace Sciences Meeting and Exhibit, Reno, Nevada, 9-12 Jan 2006. Also accepted for publication in *AIAA Journal of Thermophysics and Heat Transfer* (in press).
  22. Khan, W. A., Culham, J. R., and Yovanovich, M. M., "Optimization of Pin-Fin Heat Sinks Using Entropy Generation Minimization," *IEEE Transactions on Components and Packaging Technologies*, Vol. 28, No. 2, pp. 247-254, 2005. Also presented at ITherm 2004, Mirage Hotel and Casino, Las Vegas, NV, June 1- June 4, 2004.
  23. Kern, D. Q. and Kraus, A. D., "Extended Surface Heat Transfer," McGraw-Hill, New York, 1972.
  24. Sonn, A. and Bar-Cohen, A., "Optimum Cylindrical Pin-Fin," *Journal of Heat Transfer*, Vol. 103, pp. 814-815, 1981.
  25. Iyengar, M. and Bar-Cohen, A., "Least-Material Optimization of Vertical Pin-Fin, Plate-Fin, and Triangular-Fin Heat Sinks in Natural Convective Heat Transfer," *Proceedings of the Intersociety Conference on Thermomechanical Phenomena in Electronic Systems (ITHERM)*, May, Seattle, USA, pp. 295-302, 1998.
  26. Iyengar, M. and Bar-Cohen, A., "Least-Energy Optimization of Forced Convection Plate-Fin Heat Sinks," *Proceedings of the Intersociety Conference on Thermomechanical Phenomena in Electronic Systems (ITHERM)*, May, San Diego, California, USA, pp. 792-799, 2002.
  27. Bar-Cohen, A. and Jelinek, M., "Optimum Arrays of Longitudinal, Rectangular Fins in Convective Heat Transfer," *Heat Transfer Engineering*, Vol. 6, No. 3, pp. 68-78, 1986.
  28. Khan, W. A., "Modeling of Fluid Flow and Heat Transfer for Optimization of Pin-Fin Heat Sinks," Ph. D. Thesis, University of Waterloo, 2004.
  29. Žukauskas, A., "Heat Transfer from Tubes in Crossflow," *Advances in Heat Transfer*, Vol. 8, pp. 93-160, 1972.
  30. Stoecker, W. F., *Design of Thermal Systems*, McGraw-Hill, New York, 1989.
  31. Culham, R. J. and Muzychka, Y. S., "Optimization of Plate Fin Heat Sinks Using Entropy Generation Minimization," *IEEE Transactions on Components and Packaging Technologies*, Vol. 24, No. 2, pp. 159-165, 2001.